Journal of Medicinal Chemistry

Article

Heteroaryl-Substituted Naphthalenes and Structurally Modified Derivatives: Selective Inhibitors of CYP11B2 for the Treatment of Congestive Heart Failure and Myocardial Fibrosis

Marieke Voets, Iris Antes, Christiane Scherer, Ursula Mller-Vieira, Klaus Biemel, Catherine Barassin, Sandrine Marchais-Oberwinkler, and Rolf W. Hartmann

J. Med. Chem., **2005**, 48 (21), 6632-6642• DOI: 10.1021/jm0503704 • Publication Date (Web): 22 September 2005

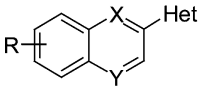

Het : 3-Pyridyl, 4-Pyridyl, 5-Pyrimidyl, 1-Imidazolyl, 5-Imidazolyl, 5-(*N*-Me)-imidazolyl, 5-oxazolyl

X : CH, N

Y : CH, N

R : H, Br, Cl, OH, OMe, OEt, OPr, OBn, CN, COOMe, $CONH_2$, CONHMe,

More About This Article

Additional resources and features associated with this article are available within the HTML version:

- Supporting Information
- Links to the 8 articles that cite this article, as of the time of this article download
- Access to high resolution figures
- Links to articles and content related to this article
- Copyright permission to reproduce figures and/or text from this article

View the Full Text HTML

Heteroaryl-Substituted Naphthalenes and Structurally Modified Derivatives: Selective Inhibitors of CYP11B2 for the Treatment of Congestive Heart Failure and Myocardial Fibrosis

Marieke Voets,[†] Iris Antes,[‡] Christiane Scherer,[†] Ursula Müller-Vieira,[†] Klaus Biemel,[§] Catherine Barassin,[§] Sandrine Marchais-Oberwinkler,[†] and Rolf W. Hartmann[†,*]

8.2 Pharmaceutical and Medicinal Chemistry, Saarland University, P.O. Box 151150, D-66041 Saarbrücken, Germany, Max Planck Institute for Informatics, Stuhlsatzenhausweg 85, D-66123 Saarbrücken, Germany, and Pharmacelsus CRO, Science Park 2, D-66123 Saarbrücken, Germany

Received April 20, 2005

Recently we proposed inhibition of aldosterone synthase (CYP11B2) as a novel strategy for the treatment of congestive heart failure and myocardial fibrosis. In this study the synthesis and biological evaluation of heteroaryl-substituted naphthalenes and quinolines (**1**−**31**) is described. Key step for the preparation of the compounds was a Suzuki cross-coupling. Activity of the compounds was determined in vitro using human CYP11B2 and selectivity was evaluated toward the human steroidogenic enzymes CYP11B1, CYP19, and CYP17. A large number of highly active and selective inhibitors of CYP11B2 was identified. The most active inhibitor was the 6-cyano compound **8** (IC_{50} = 3 nM) showing a competitive type of inhibition (K_i value = 1.9 nM). The 6-ethoxy derivative **5** was found to be the most selective CYP11B2 inhibitor (IC_{50} = 12 nM; K_i value = 8 nM; CYP11B1 IC_{50} = 5419 nM; selectivity factor = 451), showing no inhibition of human CYP3A4 (50 nM) and CYP2D6 (20 nM). Docking and molecular dynamics studies using our homology modeled CYP11B2 structure with selected compounds were performed. Caco-2 cell experiments revealed a large number of medium and highly permeable compounds and metabolic studies with **2** using rat liver microsomes showed sufficient stability.

Introduction

Aldosterone synthase (CYP11B2), a mitochondrial cytochrome P450 enzyme that is located in the adrenal cortex and to a lesser extent in the heart, brain and vascular smooth muscle cells, is the key enzyme of mineralocorticoid biosynthesis. It catalyzes the hydroxylation of 11-deoxycorticosterone to corticosterone, and two hydroxylations in the 18-position to give the most potent mineralocorticoid aldosterone.[1] This hormone is responsible for sodium retention leading to volume expansion. The adrenal aldosterone synthesis is regulated by several physiological parameters such as the renin-angiotensin-aldosterone system (RAAS) and the plasma potassium concentration. Chronic elevations in plasma aldosterone have been diagnosed in different diseases such as elevated blood pressure, congestive heart failure and myocardial fibrosis.[2,3] An insufficient renal flow stimulates the RAAS chronically, and aldosterone is released excessively. Two recent studies (RALES and EPHESUS) showed that the aldosterone antagonists spironolactone and eplerenone reduce mortality in heart failure patients and in patients after myocardial infarction.[4,5] Spironolactone, however, showed progestational and antiandrogenic side effects.[4,6] Moreover, a correlation between the use of aldosterone antagonists and hyperkalemia-associated mortality was observed.[7] After having proposed aldosterone synthase as a novel pharmacological target as early as 1994,[8] we propagated more recently the blockade of aldosterone formation by inhibition of CYP11B2 for the treatment of hyperaldosteronism, congestive heart failure and myocardial fibrosis to be a better therapeutic strategy than the use of antihormones.[9,10] Nonsteroidal inhibitors are to be preferred, for we expect these to have less side effects on the endocrine system than steroidal compounds. From our work in the field of aromatase (CYP19) and 17α-hydroxylase-C17,20-lyase (CYP17), we know that the concept of heme iron-complexing compounds is appropriate to discover highly potent and selective inhibitors.[11,12] This complexation mechanism does not only increase binding affinity of the inhibitors but also prevents oxygen activation of the heme which is required for the catalytic process. The compounds interact with the substrate binding site in the apoprotein moiety as well, which helps to increase activity and selectivity. A crucial point in the development of any CYP inhibitor is selectivity. This is especially true for CYP11B2: the inhibitors must not affect 11β-hydroxylase (CYP11B1), which is the key enzyme of glucocorticoid biosynthesis.[9,10] Selectivity toward aldosterone synthase is not easy to reach, since CYP11B1 and CYP11B2 have a sequence homology of 93%.[13] Until now, only a few compounds are known to suppress aldosterone formation. Fadrozole, an aromatase (CYP19) inhibitor which is in use for the treatment of breast cancer, reduced aldosterone and cortisol levels in vitro[14] and in vivo.[15] Ketoconazole,[16] an antimycotic and unspecific CYP inhibitor, and imidazolylmethylene-tetrahydronaphtha-

* To whom correspondence should be addressed. Phone: + 49 681 302 3424. Fax: + 49 681 302 4386. E-mail: rwh@mx.uni-saarland.de. Homepage: http://www.uni-saarland.de/fak8/hartmann/index.htm.
† Saarland University.
‡ Max Planck Institute for Informatics.
§ Pharmacelsus CRO.

10.1021/jm0503704 CCC: $30.25
Published on Web 09/22/2005

Chart 1. Compound **I** and the Title Compounds **II** Derived from **I**

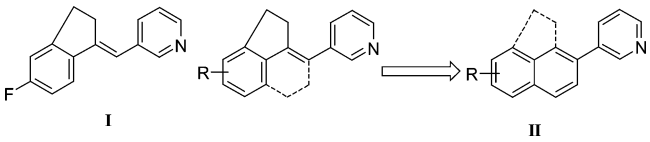

Chart 2. Title Compounds

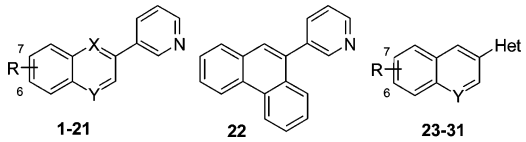

Scheme 1[a]

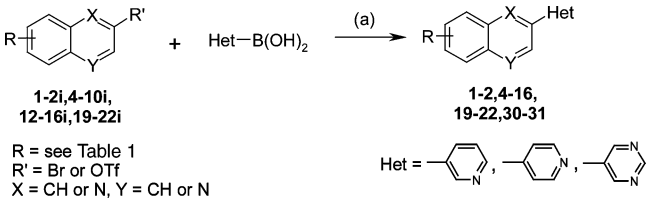

[a] Conditions: (a) Na_2CO_3, $Pd(PPh_3)_4$, DME or toluene, 4−14 h, 80 °C.

lenes and -indanes,[17] displayed moderate[16] or strong[17] inhibitory activity toward CYP11B2. However, the latter compounds showed little or no selectivity toward other CYP enzymes and therefore cannot be used in the treatment of congestive heart failure and myocardial fibrosis. Recently, we found that exchange of the imidazole ring by a pyridyl moiety increased potency and especially selectivity.[18] One of the most active inhibitors in vitro was the fluoro-substituted indane compound **I** (IC_{50} CYP11B2 = 7 nM; Chart 1) with a selectivity factor of 44 (IC_{50} CYP11B1 = 311 nM).

With the aim of further increasing activity and selectivity, we modified the structure of compound **I**. Instead of an exocyclic double bond bearing pyridylmethylene-tetrahydronaphthalenes and -indanes,[18] we synthesized a series of pyridine-substituted naphthalenes and quinolines (Chart 2). In the following paragraphs, the synthesis and the determination of their biological activity regarding inhibition of the human CYP enzymes CYP11B2, CYP11B1, CYP17 and CYP19 are described. Docking and molecular dynamics studies using our homology-modeled CYP11B2 structure[17,18] as well as determination of cell permeation properties of selected compounds using Caco-2 cells and metabolic stability of compound **2** are performed.

Chemistry

Pyri(mi)dine-substituted naphthalenes and quino(xa)lines **1**, **2**, **4**−**16**, **19**−**22**, **30**, **31** were synthesized by the route shown in Scheme 1. The key step of this synthesis was the Suzuki cross-coupling of bromo- or triflate-naphthalenes with a heteroaryl boronic acid in the presence of sodium carbonate and tetrakis(triphenylphosphine)palladium(0) as a catalyst.[19]

The bromonaphthalenes **5i**−**7i** were prepared by treating 6-bromo-2-naphthol with potassium carbonate and an alkyl halogenide.[20] The dihalogenated naphthalenes **9i** and **10i** were synthesized by reacting 2-bromo-

Scheme 2[a]

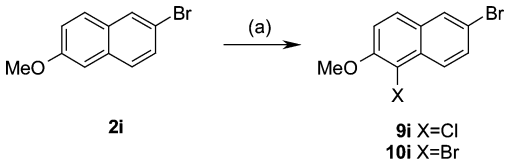

[a] Conditions: (a) NXS, THF, 3 h at reflux, 14 h at room temperature.

Scheme 3[a]

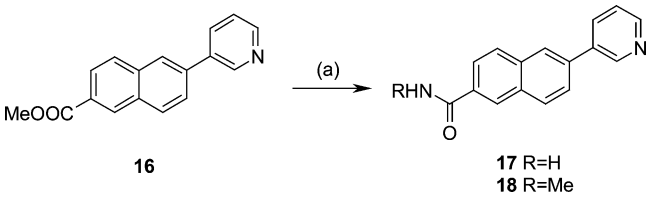

[a] Conditions: (a) RNHCHO, NaOMe, dry DMF, 1 h, 100 °C.

Scheme 4[a]

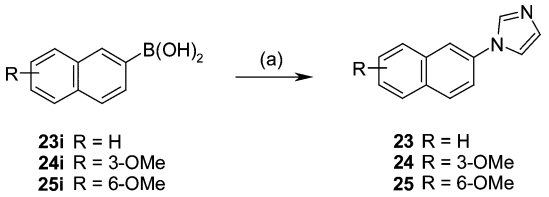

[a] Conditions: (a) imidazole, $Cu(OAc)_2$, CH_2Cl_2, 24 h, rt; or imidazole, CuI, MeOH, 2 h, reflux.

6-methoxynaphthalene **2i** with *N*-bromo- or *N*-chlorosuccinimide (Scheme 2).

To synthesize the triflates **8i**, **12i**−**14i**, the corresponding naphthols were treated with trifluoromethane sulfonic anhydride and dry pyridine at 0 °C.[21,22] The synthesis of the quinoline and quinoxaline analogues **19**−**21** started from the commercially available hydroxy quino(xa)lines. Treatment with $POBr_3$ yielded the brominated compounds **20i** and **21i**,[23] which were consecutively coupled with 3-pyridylboronic acid to give the 3-pyridylquino(xa)lines **19**−**21**.

Treatment of the methoxy-substituted naphthalene **2** with BBr_3 at −78 °C gave the hydroxy compound **3**. The conversion of the ester **16** to the amides **17** and **18** was performed in a one step reaction following a described procedure (Scheme 3).[24]

1-Imidazole-substituted naphthalenes **23**−**25** were synthesized by reacting the corresponding naphthyl boronic acids **23i**−**25i** with imidazole in the presence of a copper salt (Scheme 4).[25,26]

5-(2-Naphthyl)-1*H*-imidazole **27** was prepared by ring closure of 2-bromo-1-(2-naphthyl)ethanone **27i** with formamide following a method of Bredereck et al.[27] The reaction of tosylmethyl isocyanide (tosmic) with the *N*-methylimine **28i** or the aldehyde **29i** yielded the *N*-methylimidazole **28** or the oxazole **29**, respectively (Scheme 5).

Biological Results

Inhibition of Adrenal Corticoids Producing Human CYP11B1 and CYP11B2 in Vitro (Table 1). The inhibitory activities of the compounds toward human CYP11B2 were determined using our screening assay.[9]

Scheme 5[a]

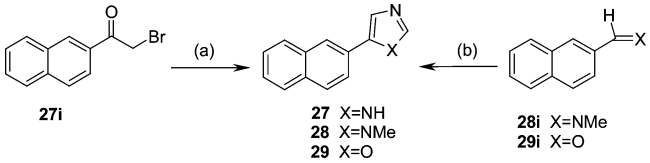

[a] Conditions: (a) NH_2CHO, 2 h, 185 °C; (b) Tosmic, K_2CO_3, MeOH, 14 h, rt.

Human CYP11B2 expressing fission yeast was incubated with [^{14}C]-deoxycorticosterone as substrate in the presence of the inhibitor at a concentration of 500 nM. The product formation was monitored by HPTLC using a phosphoimager.

Most of the 3-pyridine-substituted naphthalenes (Table 1) showed a pronounced inhibitory activity similar to or higher than the reference fadrozole (68%). The 3-methoxy and 7-methoxy compounds **15** and **13** and the quinolines **19** and **20** had only moderate activity (≈40%), while compounds **17**, **18**, **21**, and **22** showed little or no activity (<27%). Introduction of a methoxy or ethoxy group in 6-position did not change potency (**2** and **5**), but larger substituents such as propoxy diminished inhibitory activity (**6**) or resulted in complete loss of potency as shown for the benzyloxy compound **7**. The same tendency can be seen for the substituents in 5-position. The 5-chlorinated and 5-brominated compounds **9** and **10** showed high inhibitory activities, but introduction of a large 3-pyridyl substituent in the 5-position (**11**) diminished potency drastically. The shift of the methoxy substituent from the 6- into the 7-position resulted in a moderate inhibitor (**13**). However, introduction of an additional chloro substituent in the 1-position of compound **13** increased the activity significantly (**14**). 5-Pyrimidine- and 4-pyridine-substituted naphthalenes **30** and **31** showed moderate or no activity (<47%). With the exception of the unsubstituted and 3-methoxy-substituted 1-imidazolyl naphthalenes **23** and **24**, the azole-substituted compounds **25**−**29** had moderate to low potency (11−49%).

The most potent compounds, showing more than 60% inhibition in the yeast assay, as well as a few compounds with less activity were tested in V79 MZh cells expressing either human CYP11B1 or CYP11B2 to get information about activity and selectivity in mammalian cells.[9,28] The same substrate and similar conditions for incubation, extraction and analytics were used as described for the yeast assay. In Table 1 the IC_{50} values are presented. All the compounds exhibited very high activity toward CYP11B2 with IC_{50} values in the range of 3 nM to 72 nM. In addition they were highly selective by showing only little inhibition of CYP11B1 (IC_{50} = 691−10505 nM). Most of them were much more selective than the reference fadrozole which displayed a selectivity factor of 10. The most selective compounds **2** and **5** were 260-fold and 450-fold more selective for CYP11B2. Interestingly, the 5-imidazolyl compound **27** exhibited a selectivity factor of less than 1 (0.7). This is an indication that it might be possible to find selective inhibitors of CYP11B1 for the treatment of Cushing's syndrome and the metabolic syndrome as well.

Using V79 cells, compounds **5**, **8** and **12** were tested for their type of CYP11B2 inhibition. They turned out to be competitive inhibitors and revealed K_i values of 8 nM, 1.9 nM and 18 nM, respectively (K_m value deoxycorticosterone = 185 nM).

Inhibition of Human CYP19, CYP17 and Hepatic CYPs in Vitro (Table 1). Selectivity toward other steroidogenic CYP enzymes was also investigated: toward the estrogens producing CYP19 and the androgens forming CYP17. The IC_{50} values of the compounds for CYP19 were determined in vitro using human placental microsomes and [1β-^{3}H]androstenedione as substrate as described by Thompson and Siterii[29] using our modification.[30] The compounds exhibited very low to no inhibitory activity with IC_{50} values in the range between 970 nM and >36000 nM. Only compound **24** had an IC_{50} value of 129 nM, being still less potent than the reference fadrozole (IC_{50} = 30 nM).

The percent inhibition values of the compounds toward CYP17 were determined in vitro using progesterone as substrate and the 50000*g* sediment of *E.coli* recombinantly expressing human CYP17.[31,32] Most of the compounds showed a similar inhibition at a concentration of 2.5 μM as the reference ketoconazole (40%). This is not a strong effect, taking into consideration that potent CYP17 inhibitors are much more active than ketoconazole (IC_{50} ketoconazole = 4.5 μM; IC_{50} **Sa40** = 36 nM; factor = 125).[32] The 1-imidazole-substituted naphthalenes **23**, **24** and the ester **16** displayed a weaker inhibition (4−13%). The 6-methoxy- and 6-cyano-substituted naphthalenes **2** and **8** showed a higher activity toward CYP17 (IC_{50} ≈ 670 nM). The chloro-substituted compounds **12** and **14** exhibited IC_{50} values of 223 and 27 nM, respectively. Thus, the latter compound turned out to be a potent CYP17 inhibitor.

The most selective compound **5** with respect to CYP11B1 inhibition was further tested toward two crucial human hepatic CYP enzymes, CYP3A4 being responsible for 75% of the drug metabolism and CYP2D6 for which a genetic polymorphism is described. No inhibitory effects could be observed (CYP3A4, ketoconazole IC_{50} = 50 nM, **5** no inhibition at 50 nM; CYP2D6, quinidine IC_{50} = 20 nM, **5** no inhibition at 20 nM).

Computational Results. Docking and molecular dynamics studies were performed to verify our homology modeled CYP11B2 structure[17,18] and to explain very interesting structure−activity relationships of three pairs of imidazolyl and pyridyl compounds (Table 2). While in the case of the unsubstituted pyridyl and imidazolyl derivatives (**1** and **23**) both were very potent inhibitors, introduction of a OCH_3 group in the 3 or 6 position leads to a strong decrease of activity for one compound of the pairs. In case of the 3-methoxy compounds the pyridyl derivative lost activity dramatically, whereas for the 6-methoxy compounds it was the imidazolyl compound which exhibited a strong drop of activity.

After docking of the inhibitors into the protein structure, molecular dynamics simulations were performed with the inhibitor−protein complexes. In Figure 1 the docked position of the most powerful inhibitor **8** is shown (a) as well as the starting and the final positions after 1 ns of molecular dynamics of compounds **1**, **23** (b), **15** (c) and **24** (d) in the binding pocket. In pictures b−d the starting structures of the locations of the important binding pocket residues are presented. To enhance the clarity of the presentations, the final

Table 1. Inhibition of Human Adrenal CYP11B1 and CYP11B2, Human CYP17, and Human CYP19 in Vitro

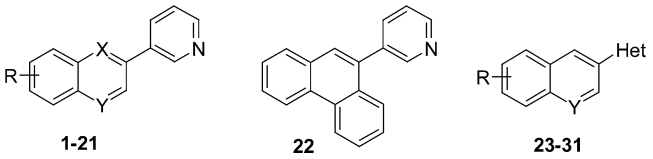

compd	R	X	Y	Het	% inhibition[a] human[b] CYP11B2	IC$_{50}$ value (nM)[c] V79 11B1[d] CYP11B1	IC$_{50}$ value (nM)[c] V79 11B2[e] CYP11B2	% inhibition[f] [IC$_{50}$ (nM)] human[g] CYP17	IC$_{50}$ value (nM)[h] human[i] CYP19	selectivity[j] factor
1	H	CH	CH		92	5826	28	40	5727	208
2	6-OMe	CH	CH		91	1577	6	72 [667]	586	263
3	6-OH	CH	CH		88	2671	23	65	>36000	116
4	6-Br	CH	CH		85	2939	15	46	>36000	196
5	6-OEt	CH	CH		86	5419	12	53	6638	451
6	6-OPr	CH	CH		36	nd	nd	nd	nd	-
7	6-OBn	CH	CH		3	nd	nd	nd	nd	-
8	6-CN	CH	CH		98	691	3	73 [686]	>36000	238
9	5-Cl-6-OMe	CH	CH		86	2517	13	32	1805	192
10	5-Br-6-OMe	CH	CH		68	4481	33	38	9107	136
11	5-(3-Pyr)−6-OMe	CH	CH		9	nd	nd	nd	nd	-
12	1,5-Cl-6-OMe	CH	CH		82	4898	28	83 [233]	970	174
13	7-OMe	CH	CH		46	nd	nd	nd	nd	-
14	1-Cl-7-OMe	CH	CH		85	2724	29	94 [27]	>36000	94
15	3-OMe	CH	CH		30	nd	nd	nd	nd	-
16	6-COOMe	CH	CH		74	10505	72	12	1252	145
17	6-CONH$_2$	CH	CH		0	nd	nd	nd	nd	-
18	6-CONHMe	CH	CH		0	nd	nd	nd	nd	-
19	H	CH	N		40	nd	nd	nd	nd	-
20	H	N	CH		53	nd	nd	nd	nd	-
21	H	N	N		13	nd	nd	nd	nd	-
22					27	7553	nd	nd	nd	-
23	H		CH	1-imidazolyl	80	1317	39	13	2821	35
24	3-OMe		CH	1-imidazolyl	87	81	19	4	129	4
25	6-OMe		CH	1-imidazolyl	49	849	218	nd	nd	4
26	H		N	1-imidazolyl	17	6338	604	nd	nd	10
27	H		CH	5-imidazolyl	41	207	296	nd	nd	0.7
28	H		CH	5-oxazolyl	11	805	12	nd	nd	66
29	H		CH	5-(N-Me)imidazolyl	28	nd	nd	nd	nd	-
30	6-OMe		CH	5-pyrimidyl	46	nd	nd	nd	nd	-
31	6-OMe		CH	4-pyridyl	0	nd	nd	nd	nd	-
ketoconazole	-	-			36	224	81	40	nd	3
fadrozole	-	-			68	10	1	5	30	10

[a] Mean value of four determinations, standard deviation less than 10%. [b] *S. pombe* expressing human CYP11B2; substrate deoxycorticosterone, 100 nM; inhibitor, 500 nM. [c] Mean value of four determinations, standard deviation less than 20%. nd = not determined. [d] Hamster lung fibroblasts expressing human CYP11B1; substrate deoxycorticosterone, 100 nM. [e] Hamster lung fibroblasts expressing human CYP11B2; substrate deoxycorticosterone, 100 nM. [f] Mean value of four determinations, standard deviation less than 10%. [g] *E. coli* expressing human CYP17; 5 mg/mL of protein; substrate progesterone, 2.5 μM; inhibitor, 2.5 μM. [h] Mean value of four determinations, standard deviation less than 5%. nd = not determined. [i] Human placental CYP19; 1 mg/mL of protein; substrate androstenedione, 500 nM. [j] IC$_{50}$ CYP11B1/IC$_{50}$ CYP11B2.

locations of the residues after the simulation are only shown if a large movement was observed (compound **15**, c). In all other cases the final positions were almost identical to the starting positions. Regarding the location of the inhibitors, the ligands remained close to the docked position except for compounds **25** (not shown) and **15** (c), the compounds which had shown little to no activity in the binding experiments. In these cases large movements were observed: at the end of the simulations the compounds had moved away from the heme and the Fe−N (ligand) contact was broken (Table 2).

Obviously the activities of the compounds strongly depend on their geometrical properties. In the series of 6-methoxy-substituted compounds, activity correlates with the angle between the Fe−N bond and the naphthyl-aryl C−C bond. In case of the highly active 3-pyridyl compound **2** the angle is 120°, whereas it is 144° for the imidazolyl compound **25** which is clearly less active and 180° for the inactive 4-pyridyl compound. Stretching of the angle in this series of compounds leads to unfavorable interactions resulting in inactivity.

To gain a deeper insight into these phenomena the binding modes of the compounds in the original docking positions were studied. One major difference was observed for compound **15** in comparison to the other compounds. The requirement for a strong inhibitor binding is an Fe−N interaction which is almost perpendicular with respect to the plane of the heme. In the case of compound **15** this leads to positions much closer to the I-helix (partially shown in Figure 1: Val316−Thr319) than observed for the other inhibitors. These positions are obviously energetically unfavorable because the hydrophilic/hydrophobic regions in the I-helix are located close to the aromatic regions of the ligands. Thus, during the simulation, the compounds, while minimizing unfavorable contacts, reorient themselves and subsequently lose contact with the heme group (Table 2).

Table 2. IC_{50} Values for CYP11B2 Inhibition and Fe(heme)-N(inhibitor) Distances after Docking and Molecular Dynamics of Selected Compounds[a]

Compd	Structure	IC_{50}-value (nM) V79 11B2 / CYP11B2	Fe-N distance (Å) after docking	Fe-N distance (Å) after MD[a]
1	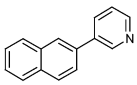	28.4	2.48	2.63
23	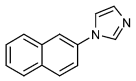	38.5	2.38	2.13
2	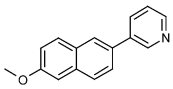	6.2	2.27	2.48
25	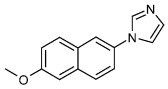	218.0	2.29	7.36
15	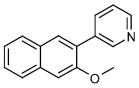	>500	2.52	10.58
24	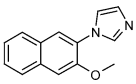	19.1	2.08	2.52

[a] Time for MD simulations: 1ns.

In addition it was observed that in the case of compound **24** the methoxy group fits perfectly into a hydrophobic groove formed by the amino acid residues of Thr318 (CH_3 group), Arg490 (CH_2−CH_2 chain), and Pro491 as shown on the right side of Figure 1d. In case of compound **15** the larger size of the pyridyl ring and especially the different geometry of the complex due to the binding of the nitrogen to the heme prohibits the methoxy group from fitting into this pocket. Thus, the methoxy group is turned by nearly 180°, leading to the above-described unfavorable position of the inhibitor.

Permeability Screening using Caco-2 Monolayers. Selected compounds (**1**−**4**, **8**−**10**, **12**, **14**, **16**, **23**), which showed high activity and selectivity, were further examined for peroral absorption using Caco-2 monolayers. These cells exhibit morphological and physiological properties of the human small intestine[33] and are generally accepted to be an appropriate model for the prediction of intestinal absorption in vivo.[34] To increase the throughput of the assay, a multiple dosing approach was employed for the test compounds. The applicability of compound mixture administration was demonstrated for **1**, **2** and **12** in comparison to single dosing (single dosing P_{app} (10^{-6} cm/s) ± SD: **1**, 5.5 ± 0.5, **2**, 9.0 ± 0.3, **12**, 2.1 ± 0.1; multiple dosing: see Table 3). Using this approach, compounds can be classified as low (P_{app} (10^{-6} cm/s) < 1), medium (1 < P_{app} (10^{-6} cm/s) < 10) or highly (P_{app} (10^{-6} cm/s) > 10) permeable. Most of the tested compounds were medium to highly permeable. Only the halogenated naphthalenes (**4**, **9**, **10**, **14**) had a lower permeability. The ester **16**, on the other hand, was not permeable at all (Table 3).

Additionally, the logP values of the test compounds and their solubilities in water were calculated as these parameters are often correlated with absorption. All the inhibitors had logP values in the range between 3.1 and 4.7 and solubility values in the range of 2.8×10^{-4} and 1.3×10^{-6} mol/L at pH 7.4 (Table 3). Interestingly, the highly permeable inhibitors **3**, **8** and **23** showed low logP values and high solubility values whereas the medium and low permeators exhibited higher logP values and lower solubilities.

Metabolic Stability. Because of its high activity and selectivity and its favorable permeability properties, the 6-methoxy naphthalene **2** was selected to be further tested for metabolic stability in rat liver microsomes. Samples were taken at various time points and the remaining percentage of parent compound was determined. Compound **2** showed a half-life of 93 min, which is an indication that its metabolic stability is sufficient. In a next step, the major metabolites of compound **2** were investigated using LC-MS/MS (Figure 2). The fragmentation of the metabolite with the $[M + H]^+$ at *m/z* 222 suggests that **2** has undergone O-demethylation resulting in the formation of the corresponding naphthol **3**. Two other major metabolites with the $[M + H]^+$ at *m/z* 252 bear an additional oxygen in their (6-methoxy-2-naphthyl)pyridine core structure.

Discussion and Conclusion

Selectivity is a crucial point for the use of drugs in general. This is especially true for the treatment of congestive heart failure and myocardial fibrosis. The aldosterone receptor antagonist spironolactone shows progestational and antiandrogenic side effects because of insufficient selectivity toward the aldosterone receptor.[4,6] Fadrozole, which lowers aldosterone and cortisol levels after application of a dose 10-fold higher than the therapeutical dose,[13] is used as aromatase (CYP19) inhibitor for the therapy of breast cancer and is therefore not appropriate for the therapy of cardiovascular diseases. For inhibitors of corticoid biosynthesis, selectivity is definitely an extremely important issue since CYP11B1 and CYP11B2 are for more than 93% identical at the protein level.[13] Imidazolylmethylene-tetrahydronaphthalenes and -indanes showed only moderate selectivity toward CYP11B2.[17] The pyridylmethylene-tetrahydronaphthalenes and -indanes, also recently described by us,[18] turned out to be potent and selective CYP11B2 inhibitors. Aiming at the discovery of a class of highly active and even more selective inhibitors of aldosterone synthase, we modified the lead compound **I** and synthesized a series of heteroaryl-substituted naphthalenes and nitrogen bearing analogues.

The structure−activity relationships obtained revealed that the naphthalene core is more appropriate than the (iso)quinoline or quinoxaline moiety, since the latter compounds **19**−**21** and **26** showed low or no activity. Obviously a nitrogen atom at this position is unfavorable for an optimal interaction with the active site. On the other hand, an important structural feature of CYP inhibitors is a nitrogen-containing heterocyclic substituent at the core molecule which can complex with the heme iron. The results presented in this paper show that the 3-pyridyl moiety is ideal with respect to activity and selectivity. The replacement of this group by other heterocycles resulted in a decrease or loss of activity in most cases. Only the 1-imidazole-substituted compounds **23** and **24** were very active, but their selectivity was low. Substitution in the 6-position of the naphthalene ring is appropriate for high activity and selectivity. Only in case of space-filling substituents, like propoxy or

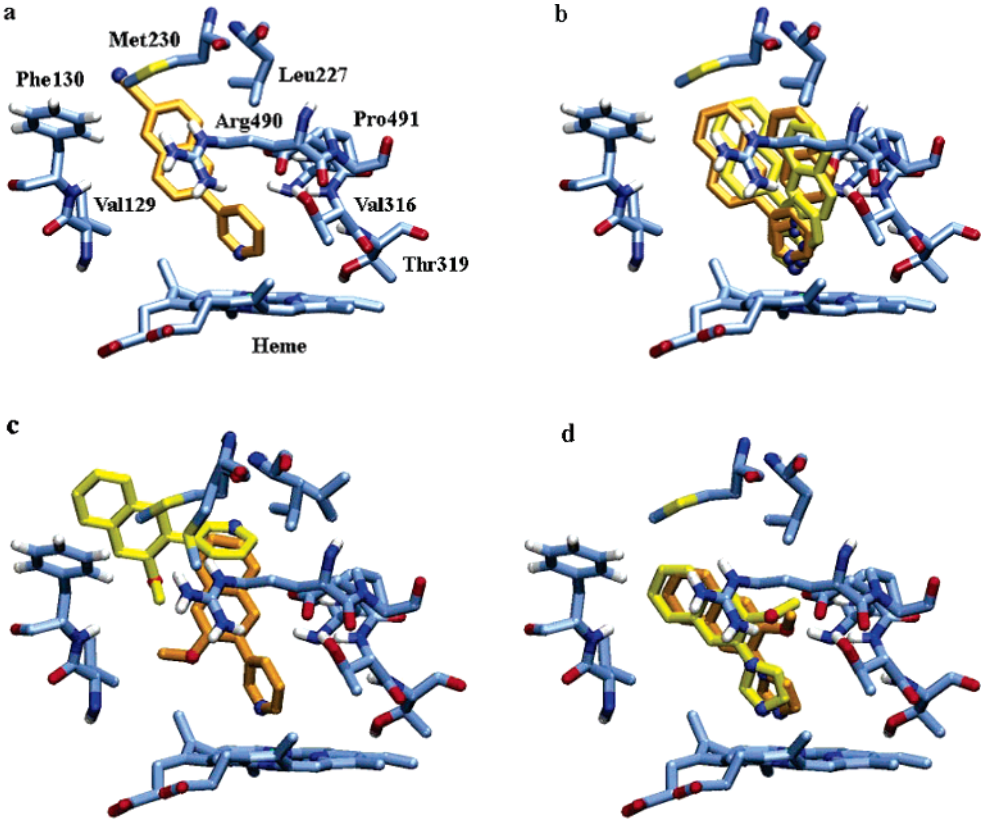

Figure 1. Selected residues of the energy minimized structures of CYP11B2 complexed with the compounds **8** (a), **1**, **23** (b), **15** (c) and **24** (d). For the inhibitors, the starting (orange) and end (yellow) positions of the MD simulations are shown. In part c, the end conformations of Met230 and Leu227 are also given.

Table 3. Caco-2 Cell Permeation of Highly Active and Selective Compounds Using a Multiple Dosing Approach

compd	P_{app} (10^{-6} cm/s)[a,b] multiple dosing ± SD	logP[c]	solubility (mol/L)[c,d]
1	2.9 ± 0.7	3.89 ± 0.24	2.0×10^{-4}
2	7.9 ± 0.6	3.81 ± 0.26	7.9×10^{-5}
3	17.4 ± 1.0	3.15 ± 0.25	2.3×10^{-4}
4	1.2 ± 0.1	4.66 ± 0.34	1.3×10^{-6}
8	10.8 ± 0.4	3.33 ± 0.29	1.6×10^{-4}
9	1.5 ± 0.1	4.35 ± 0.36	7.6×10^{-6}
10	1.0 ± 0.3	4.38 ± 0.37	3.9×10^{-5}
12	2.2 ± 0.3	4.71 ± 0.42	7.2×10^{-6}
14	0.5 ± 0.05	4.28 ± 0.28	1.4×10^{-5}
16	0	3.87 ± 0.26	7.1×10^{-5}
23	14.7 ± 0.6	3.21 ± 0.57	2.8×10^{-4}
atenolol	0.1 ± 0.03		
ketoprofene	25.7 ± 0.5		
testosterone	9.4 ± 0.2		
erythromycin	< LOD		

[a] Permeability of research compounds was classified according to well described reference compounds: atenolol,[35] ketoprofene,[36] testosterone[37] and erythromycin.[37] [b] Mean value of three determinations. [c] Calculated with ACD/I-lab. [d] At pH 7.4.

benzyloxy (**6**, **7**), the activity drops drastically. Further substitution in the 5-position did not result in lower potency, provided that this substituent was not too large as for compound **11**. A loss in activity was observed for compounds with substituents in 3- or 7-position (**13**, **15**).

In this study, we demonstrated that 3-pyridine-substituted naphthalenes showed in vitro a highly selective inhibition of CYP11B2 versus CYP11B1, despite the high homology between the two enzymes. These compounds showed even better selectivity profiles than the (pyridylmethylene)tetrahydronaphthalenes and -indanes.[18] The best 3-pyridyl compounds described in this paper exhibited selectivity factors for CYP11B2 exceeding 190 (**1**, **2**, **4**, **8**). In the case of the 6-ethoxy compound **5** an exceptional 451-fold stronger inhibition of CYP11B2 compared to CYP11B1 was observed. Additionally, the sex hormone-synthesizing enzymes CYP17 and CYP19 and the drug-metabolizing enzymes CYP3A4 and CYP2D6 were not affected at all.

The results of the molecular dynamics studies showed that for the highly potent compounds **1**, **2**, **23** and **24**, the docked positions remained stable throughout the simulations. For the two less potent compounds **15** and **25**, however, major rearrangements of the inhibitors in the complex were observed leading to the breaking of their Fe−N interactions. A closer analysis of the ligand interactions with the binding pocket revealed that in the case of **15** and **25** the formation of a close Fe−N interaction leads to unfavorable contacts between the ligands and the I-helix of the protein. As it is known that a strong Fe−N interaction is a prerequisite for strong inhibitor binding, it can be concluded that the reason for the small inhibitory potency of **15** and **25** is mainly steric. In addition, this study shows that the protein model[38] of CYP11B2, which has been improved continuously,[17,18] demonstrates some predictive value now.

As the in vivo applicability of in vitro active and selective compounds is often hampered by unfavorable pharmacokinetics, in vitro experiments for the prediction of permeability and metabolic properties were performed. Caco-2 cells were used for the prediction of peroral absorption. Permeability screening of some potent and selective compounds showed that the unsubstituted (**1**, **23**) and the 6-substituted naphthalenes

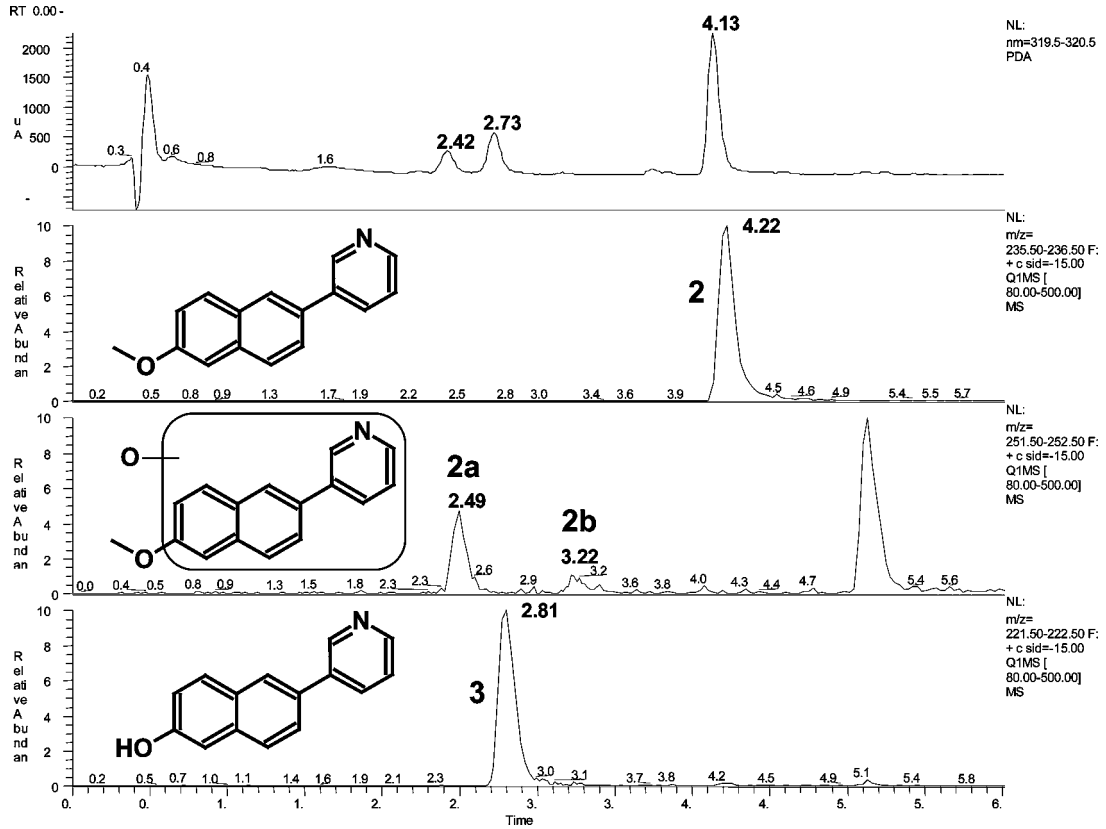

Figure 2. Representative UV (230 nm) and product ion MS/MS chromatograms of compound **2** and its putative metabolites (**2a**,**b** and **3**) detected in rat liver microsomes incubated for 180 min.

(**2**, **3**, **8**) were medium to highly permeable. When halogens were introduced into the naphthalene core, the permeability dropped substantially (**4**, **9**, **10**, **12**, **14**). An ester group at the naphthalene ring led to a complete loss of permeability (**16**).

The metabolic stability of the highly permeable compound **2** was subsequently investigated using liver microsomes. With a half-life of 93 min, the 6-methoxy compound **2** is metabolically sufficiently stable. Its major metabolites were examined by mass spectrometry. The demethylated and two hydroxylated compounds could be identified and can be assumed to be substrates for further phase-II-deactivation followed by renal clearance.

Two physicochemical parameters have a substantial influence on drug properties: i.e., aqueous solubility, which is critical to drug delivery, and lipophilicity (logP), which plays a key role in drug absorption, transport and distribution. The aqueous solubility of the very potent and selective compounds **1**−**5**, **8**−**10** and **12** was in the range between 1.3×10^{-6} and 2.3×10^{-4} mol/L. All the inhibitors exhibited favorable logP values lower than 5, except the benzyloxy compound **7**. The most potent CYP11B2 inhibitor **8** had a logP value of 3.3 and a solubility of 1.6×10^{-4} mol/L.

In conclusion, we have developed a new class of highly active and selective inhibitors of CYP11B2 by structurally modifying the lead compound **I**. The most active CYP11B2 inhibitor was the 6-cyano compound **8** ($IC_{50} = 3$ nM). The 6-ethoxy compound **5** turned out to be a very active ($IC_{50} = 12$ nM) and the most selective inhibitor showing a selectivity factor of 451. Taking pharmacokinetic properties into consideration, the 6-methoxy compound **2** seems to be very promising for in vivo application, Presently, in vivo studies are being performed to investigate the plasma aldosterone levels. Provided that in vivo activity is confirmed, these compounds could offer a new therapeutic option for the treatment of congestive heart failure and myocardial fibrosis.

Experimental Section

Chemical Methods. Melting points were measured on a Mettler FP1 melting point apparatus and are uncorrected. IR spectra were measured neat on a Bruker Vector 33FT-infrared spectrometer. ^{1}H NMR spectra were recorded on a Bruker DRX-500 (500 MHz) instrument. Chemical shifts are given in parts per million, and TMS was used as internal standard for spectra obtained in $CDCl_3$. All coupling constants (J) are given in Hz. Mass spectra (electrospray ionization (ESI)) were measured on a TSQ Quantum (Thermo Electron Corporation) instrument. Elemental analyses were performed at the department of Instrumental Analysis and Bioanalysis, University of the Saarland. Reagents and solvents were used as obtained from commercial suppliers without further purification. Column chromatography (CC) was performed using silica gel (70−200 μm), and the reaction progress was determined by TLC analyses on ALUGRAM SIL G/UV_{254} (Macherey-Nagel).

The following compounds were prepared according to previously described procedures: 6-cyano-2-naphthyl trifluoromethanesulfonate (**8i**),[21] 1,5-dichloro-6-methoxy-2-naphthalen-2-ol (**12ii**),[22] 1,5-dichloro-6-methoxy-2-naphthyl trifluoromethanesulfonate (**12i**),[22] 7-methoxy-2-naphthyl trifluoromethanesulfonate (**13i**),[22] 2-methoxy-3-naphthylboronic acid (**15i**),[39] 3-pyridylboronic acid,[40] 4-pyridylboronic acid,[40] 5-pyrimidylboronic acid,[40] 2-bromoquinoline (**20i**),[23] 1-(3-methoxy-2-naphthyl)-1*H*-imidazole (**24**),[26] 3-imidazol-1-yl-quinoline (**26**),[41] 2-bromo-1-(2-naphthyl)ethanone (**27i**),[42] methylnaphthalen-2-ylmethylenamine (**28i**).[43]

General Procedure for the Synthesis of Compounds (1−2, 4−9, 12−14, 16, 19−22). A mixture of substituted 2-bromo- or 2-trifluoromethanesulfonate compound (1.50 mmol), 3-pyridylboronic acid (1.95 mmol), aqueous Na_2CO_3 (3.15 mmol) and $Pd(PPh_3)_4$ (0.03 mmol) in 15 mL of ethylene glycol dimethyl ether or toluene was stirred overnight at 80 °C under nitrogen. The reaction was cooled to room temperature, and water was added. The mixture was extracted with ethyl acetate, dried ($MgSO_4$), filtered and evaporated in vacuo.

3-(2-Naphthyl)pyridine (1). Purification: CC (CH_2Cl_2/MeOH, 97:3). Yield 82%, mp 101 °C. ^{1}H NMR ($CDCl_3$): δ 7.43−7.45 (m, 1H, Pyr. H-5), 7.51−7.56 (m, 2H, Ar H), 7.71 (dd, 1H, ^3J = 8.5 Hz, ^4J = 1.6 Hz, Ar H), 7.88−7.90 (m, 2H, Ar H), 7.96 (d, 1H, ^3J = 8.5 Hz, Ar H), 8.03−8.05 (m, 2H, Ar H, Pyr. H-4), 8.63 (dd, 1H, ^3J = 4.7 Hz, ^4J = 1.6 Hz, Pyr. H-6), 8.99 (dd, 1H, ^4J = 1.6 Hz, Pyr. H-2). IR cm^{-1}: ν_{max} 3392, 3051, 3029, 1599, 1484. MS *m/z* 206 (MH$^+$), 178, 151, 77, 51. Anal. ($C_{15}H_{11}N\cdot0.04H_2O$) C, H, N.

3-(6-Methoxy-2-naphthyl)pyridine (2). Purification: CC (CH_2Cl_2/MeOH, 97:3). Yield 77%, mp 120 °C. ^{1}H NMR ($CDCl_3$): δ 3.95 (s, 1H, OCH_3), 7.17 (d, 1H, ^4J = 2.5 Hz, Ar H), 7.22 (dd,1H, ^3J = 8.8 Hz, ^4J = 2.2 Hz, Ar H), 7.45−7.47 (m, 1H, Pyr. H-5), 7.67 (dd, 1H, ^3J = 8.5 Hz, ^4J = 1.8 Hz, Ar H), 7.81 (d, 1H, ^3J = 8.5 Hz, Ar H), 7.85 (d, 1H, ^3J = 8.5 Hz, Ar H), 7.98 (s, 1H, Ar H), 8.04−8.06 (m, 1H, Pyr. H-4), 8.61 (dd, 1H, ^3J = 4.7 Hz, ^4J = 1.3 Hz, Pyr. H-6), 8.97 (s, 1H, Pyr. H-2). IR cm^{-1}: ν_{max} 3058, 2938, 1605, 1489. MS *m/z* 236 (MH$^+$). Anal. ($C_{16}H_{13}NO\cdot0.04H_2O$) C, H, N.

Synthesis of 6-Pyridin-3-ylnaphthalen-2-ol (3). BBr_3 (2.55 mL, 2.55 mmol) was slowly added to compound **2** (150 mg, 0.64 mmol) in 25 mL of dry CH_2Cl_2 at −78 °C under nitrogen atmosphere. After 30 min stirring, the cooling was stopped and the reaction was stirred at room temperature overnight. The reaction was slowly quenched with methanol and then washed with a saturated $NaHCO_3$ solution. The organic layer was dried ($MgSO_4$), filtered and evaporated in vacuo. The product was purified by column chromatography, eluting with CH_2Cl_2/MeOH (99:1). Yield 65%, mp 253 °C. ^{1}H NMR ($CDCl_3$): δ 7.20 (dd, 1H, ^3J = 8.8 Hz, ^4J = 1.9 Hz, Ar H), 7.23 (d, 1H, ^4J = 1.9 Hz, Ar H), 7.60−7.62 (m, 1H, Pyr. H-5), 7.83 (dd, 1H, ^3J = 8.5 Hz, ^4J = 1.6 Hz, Ar H), 7.87 (d, 1H, ^3J = 8.8 Hz, Ar H), 7.92 (d, 1H, ^3J = 8.8 Hz, Ar H), 8.24 (s, 1H, Ar H), 8.29 (dt, 1H, ^3J = 7.9 Hz, ^4J = 1.9 Hz, Pyr. H-4), 8.65 (d, 1H, ^3J = 4.7 Hz, Pyr. H-6), 9.08 (d, 1H, ^4J = 1.6 Hz, Pyr. H-2), 9.95 (s, 1H, OH). IR cm^{-1}: ν_{max} 3634, 3021, 1594, 1489, 1308, 793. MS *m/z* 222 (MH$^+$). Anal. ($C_{15}H_{11}NO\cdot0.24H_2O$) C, H, N.

Synthesis of 3-(5-Bromo-6-methoxy-2-naphthyl)pyridine (10) and 3,3′-(2-Methoxynaphthalene-1,6-diyl)dipyridine (11). A mixture of 1,6-dibromo-2-methoxynaphthalene **10i** (223 mg, 0.71 mmol), 3-pyridylboronic acid (0.26 g, 2.12 mmol), Na_2CO_3 (0.30 g, 2.82 mmol) and $Pd(PPh_3)_4$ (16 mg) in ethylene glycol dimethyl ether was stirred overnight at 80 °C under nitrogen. The reaction was cooled to room temperature, and water was added. The mixture was extracted with ethyl acetate, dried ($MgSO_4$), filtered and evaporated in vacuo. The mixture of compounds **10** and **11** was purified by column chromatography, eluting with CH_2Cl_2/MeOH (98:2).

3-(5-Bromo-6-methoxy-2-naphthyl)pyridine (10). Yield 66%, mp 162 °C. ^{1}H NMR ($CDCl_3$): δ 4.07 (s, 3H, OCH_3), 7.36 (d, 1H, ^3J = 8.8 Hz, Ar H), 7.60−7.63 (m, 1H, Pyr. H-5), 7.79 (dd, 1H, ^3J = 8.8 Hz, ^4J = 2.2 Hz, Ar H), 7.92 (d, 1H, ^3J = 8.8 Hz, Ar H), 8.02 (d, 1H, ^4J = 1.9 Hz, Ar H), 8.22 (dt, 1H, ^3J = 7.9 Hz, ^4J = 2.2 Hz, Pyr. H-4), 8.36 (d, 1H, ^3J = 8.8 Hz, Ar H), 8.65 (dd, 1H, ^3J = 5.0 Hz, ^4J = 1.6 Hz, Pyr. H-6), 9.01 (d, 1H, ^4J = 2.2 Hz, Pyr. H-2). IR cm^{-1}: ν_{max} 3045, 2955, 2832, 1601, 1488, 1272. MS *m/z* 317−314 (MH$^+$), 270, 227, 191, 163. Anal. ($C_{16}H_{12}NO$) C, H, N.

3,3′-(2-Methoxynaphthalene-1,6-diyl)dipyridine (11). Yield 5%, mp 173 °C. ^{1}H NMR ($CDCl_3$): δ 3.89 (s, 3H, OCH_3), 7.43−7.46 (m, 2H, Ar H, Pyr. H-5), 7.54−7.56 (m, 2H, Ar H, Pyr. H-5), 7.62 (dd, 1H,^3J = 8.8 Hz, ^4J = 1.9 Hz, Ar H), 7.86 (dt, 1H, ^3J = 7.9 Hz, ^4J = 1.9 Hz, Pyr. H-4), 8.01−8.04 (m, 2H, Ar H, Pyr.H-4), 8.07 (d, 1H, ^4J = 1.6 Hz, Ar H), 8.62 (d, 1H, ^3J = 5.0 Hz, Pyr. H-6), 8.68 (s, 1H, Pyr. H-2), 8.70 (d, 1H, ^3J = 5.0 Hz, Pyr. H-6), 8.97 (s, 1H, Pyr. H-2). IR cm^{-1}: ν_{max} 3031, 2950, 2842, 1599, 1488, 1258. MS *m/z* 313 (MH$^+$).

Synthesis of 3-(3-Methoxy-2-naphthyl)pyridine (15). A mixture of 3-bromopyridine (0.20 g, 1.25 mmol), 2-methoxy-3-naphthylboronic acid (0.30 g, 1.50 mmol), aqueous Na_2CO_3 (0.27 g, 2.50 mmol) and $Pd(PPh_3)_4$ (30 mg) in 15 mL of ethylene glycol dimethyl ether was stirred at 90 °C for 4 h and at room-temperature overnight. Water was added, and the mixture was extracted with dichloromethane, dried ($MgSO_4$), filtered and evaporated in vacuo. The product was purified by column chromatography, eluting with CH_2Cl_2/MeOH (98:2). Yield 31%, mp 189 °C. ^{1}H NMR ($CDCl_3$): δ 3.94 (s, 3H, OCH_3), 7.25 (s, 1H, Ar H), 7.35−7.40 (m, 2H, Ar H, Pyr. H-5), 7.48 (td, 1H, ^3J = 8.2 Hz, ^4J = 1.3 Hz, Ar H), 7.77 (s, 1H, Ar H), 7.78 (d, 1H, ^3J = 8.2 Hz, Ar H), 7.81 (d, 1H, ^3J = 8.2 Hz, Ar H), 7.93 (dt, 1H, ^3J = 7.9 Hz, ^4J = 1.9 Hz, Pyr. H-4), 8.60 (dd, 1H, ^3J = 4.9 Hz, ^4J = 1.8 Hz, Pyr. H-6), 8.85 (s, 1H, Pyr. H-2). IR cm^{-1}: ν_{max}. 3054, 2962, 2832, 1631, 1599, 1504, 1466, 1410, 1254. MS *m/z* 236 (MH$^+$). Anal. ($C_{16}H_{13}NO\cdot HCl\cdot0.26H_2O$) C, H, N.

General Procedure for the Synthesis of Compounds (17, 18). A stirred mixture of compound **16** (0.60 mmol) and formamide (1.90 mmol) under nitrogen was charged with anhydrous DMF (2 mL) and heated at 100 °C. Methanolic sodium methoxide (0.40 mmol) was added, and stirring was continued for 1 h. The mixture was cooled and water was added (2 mL), then extracted with ethyl acetate, dried ($MgSO_4$), filtered and evaporated in vacuo. The product was purified by column chromatography, eluting with CH_2Cl_2/MeOH (95:5).

6-Pyridin-3-yl-2-naphthamide (17). Yield 61%, mp 227 °C. ^{1}H NMR ($CDCl_3$): δ 7.42−7.45 (m, 1H, Pyr. H-5), 7.75 (dd, 1H, ^3J = 8.5 Hz, ^4J = 1.9 Hz, Ar H), 7.90 (dd, 1H, ^3J = 8.5 Hz, ^4J = 1.9 Hz, Ar H), 7.96 (d, 1H, ^3J = 8.8 Hz, Ar H), 8.01−8.04 (m, 2H, Ar H, Pyr. H-4), 8.06 (d, 1H, ^4J = 1.3 Hz, Ar H), 8.38 (d, 1H, ^4J = 1.3 Hz, Ar H), 8.59 (dd, 1H, ^3J = 4.7 Hz, ^4J = 1.6 Hz, Pyr. H-6), 8.92 (d, 1H, ^4J = 1.9 Hz, Pyr. H-2). IR cm^{-1}: ν_{max}.3335, 3066, 1664, 1590, 1426. MS *m/z* 249 (MH$^+$). Anal. ($C_{16}H_{12}NO$) C, H, N.

***N*-Methyl-6-pyridin-3-yl-2-naphthamide (18).** *N*-Methylformamide was used instead of formamide. Yield 83%, mp 158 °C. ^{1}H NMR ($CDCl_3$): δ 3.10 (s, 3H, OCH_3), 6.33 (s, 1H, NH), 7.42−7.44 (m, 1H, Pyr. H-5), 7.77 (dd, 1H, ^3J = 8.5 Hz, ^4J = 1.8 Hz, Ar H), 7.87 (dd, 1H, ^3J = 8.5 Hz, ^4J = 1.8 Hz, Ar H), 7.96−8.07 (m, 4H, Ar H, Pyr. H-4), 8.33 (s, 1H, Ar H), 8.65 (dd, 1H, ^3J = 4.6 Hz, ^4J = 1.5 Hz, Pyr. H-6), 8.98 (d, 1H, ^4J = 1.5 Hz, Pyr. H-2). IR cm^{-1}: ν_{max} 3316, 3059, 2929, 1644, 1549, 1313. MS *m/z* 263 (MH$^+$). Anal. ($C_{17}H_{14}N_2O\cdot0.15H_2O$) C, H, N.

General Procedure for the Synthesis of Compounds (23, 25).[25] A mixture of 2-naphthylboronic acid (1.00 mmol), imidazole (0.50 mmol), copper(II) acetate (0.75 mmol), pyridine (1.00 mmol) and 4 Å molecular sieve in 6 mL of anhydrous dichloromethane was stirred at room temperature for 2 days. The mixture was filtered and evaporated in vacuo. The product was purified by chromatography, eluting with CH_2Cl_2/MeOH (99:1).

1-(2-Naphthyl)-1*H*-imidazole (23). Yield 34%, mp 123 °C. ^{1}H NMR ($CDCl_3$): δ 7.26 (s, 1H, Im. H-4), 7.40 (s, 1H, Im. H-5), 7.51−7.58 (m, 3H, Ar H), 7.82 (d, 1H, ^4J = 1.5 Hz, Ar H), 7.88 (t, 2H, ^3J = 7.6 Hz, Ar H), 7.96 (d, 1H, ^3J = 7.6 Hz, Ar H), 8.05 (s, 1H, Im. H-2). IR cm^{-1}: ν_{max}. 3116, 3058, 1688, 1602, 1493. MS *m/z* 195 (MH$^+$), 167, 139, 115, 77, 51. Anal. ($C_{13}H_{10}N_2\cdot0.08H_2O$) C, H, N.

1-(6-Methoxynaphthalen-2-yl)-1*H*-imidazole (25). Yield 13%, mp 85 °C. ^{1}H NMR ($CDCl_3$): δ 3.95 (s, 3H, OCH_3), 7.18 (d, 1H, ^4J = 2.5 Hz, Ar H), 7.24 (dd, 1H, ^3J = 8.5 Hz, ^4J = 2.5 Hz, Ar H), 7.28 (s, 1H, Im. H-4), 7.38 (s, 1H, Im. H-5), 7.48 (dd, 1H, ^3J = 8.5 Hz, ^4J = 2.5 Hz, Ar H), 7.76 (s, 1H, Ar H), 7.77 (d, 1H, ^3J = 8.5 Hz, Ar H), 7.85 (d, 1H, ^3J = 8.5 Hz, Ar H), 8.07 (s, 1H, Im. H-2). IR cm^{-1}: ν_{max}. 3113, 3003, 2962, 2842,

1607. MS *m/z* 225 (MH^+), 210, 126. Anal. ($C_{14}H_{12}N_2O \cdot 0.13H_2O$) C, N; H: calcd, 5.45; found, 5.96.

Synthesis of 5-(2-Naphthyl)-1*H*-imidazole (27).[26] A solution of 2-bromo-1-(2-naphthyl)ethanone **27i** (0.5 g, 2.01 mmol) in 2.4 mL of formamide was stirred at 185 °C for 2 h. After cooling, the mixture was poured into 12 mL of hot, diluted HCl solution and active charcoal was added. After stirring for 15 min, the mixture was filtered and basified with an aqueous ammonia solution and extracted with ethyl acetate. The organic layer was dried ($MgSO_4$), filtered and evaporated in vacuo. The product was purified by chromatography, eluting with CH_2Cl_2. Yield 9%, mp 171 °C. ^{1}H NMR ($CDCl_3$): δ 7.38 (s, 1H, Im. H-4), 7.39−7.45 (m, 2H, Ar H), 7.73 (dd, 1H, ^3J = 8.5 Hz, ^4J = 1.9 Hz, Ar H), 7.74−7.81 (m, 4H, Ar H, Im. H-2), 8.13 (s, 1H, Ar H). IR cm^{-1}: ν_{max} 3125, 3044, 2852. MS *m/z* 195 (MH^+), 168, 141. Anal. ($C_{13}H_{10}N_2 \cdot 0.05H_2O$) C, H, N.

General Procedure for the Synthesis of Compounds (28, 29). A mixture of **28i** or **29i** (3 mmol), tosylmethyl isocyanide (3 mmol) and K_2CO_3 (3 mmol) in 25 mL of absolute methanol was stirred at room-temperature overnight. Methanol was evaporated in vacuo and dichloromethane was added to the crude product. After washing with water, the organic layer was dried ($MgSO_4$), filtered and evaporated in vacuo. The product was purified by chromatography, eluting with CH_2Cl_2/MeOH (97:3).

1-Methyl-5-(2-naphthyl)-1*H*-imidazole (28). Yield 18%, mp 103 °C. ^{1}H NMR ($CDCl_3$): δ 3.75 (s, 3H, CH_3), 7.22 (s, 1H, Im. H-4), 7.49−7.53 (m, 3H, Ar H), 7.68 (s, 1H, Im. H-2), 7.85−7.87 (m, 3H, Ar H), 7.91 (d, 1H, ^3J = 8.5 Hz, Ar H). IR cm^{-1}: ν_{max} 3083, 3053, 2952, 1600, 1490. MS *m/z* 209 (MH^+), 167, 139, 115. Anal. ($C_{14}H_{12}N_2 \cdot 0.19H_2O$) C, H, N.

5-(2-Naphthyl)-1,3-oxazole (29). Yield 28%, mp 121 °C. ^{1}H NMR ($CDCl_3$): δ 7.47 (s, 1H, Im. H-4), 7.49−7.54 (m, 2H, Ar H), 7.73 (dd, 1H, ^3J = 8.5 Hz, ^4J = 1.6 Hz, Ar H), 7.83−7.90 (m, 3H, Ar H), 7.97 (s, 1H, Im. H-2), 8.14 (s, 1H, Ar H). IR cm^{-1}: ν_{max} 3128, 3055, 2952, 1630, 1497. MS *m/z* 196 (MH^+), 167, 139, 115. Anal. ($C_{13}H_9NO \cdot 0.08H_2O$) C, H, N.

Biological Methods. 1. Enzyme Preparations. CYP17 and CYP19 preparations were obtained using described methods: the 50 000*g* sediment of *E. coli* expressing human CYP17[32] and microsomes from human placenta for CYP19.[30]

2. Enzyme Assays. The following enzyme assays were performed as previously described: CYP17[32] and CYP19.[30]

3. Screening Assay in Fission Yeast. To test the inhibitory activity of compounds toward human CYP11B2, fission yeast *Schizosaccheromyces pombe* PE1, recombinantly expressing the target enzyme, was used. A fission yeast suspension (diluted to cellular density 3×10^7 cells/mL) was prepared from a freshly grown culture using a modified EMMG medium at pH 7.4. A 500 μL aliquot of the yeast suspension was preincubated with the potential inhibitor dissolved in ethanol, in a final concentration of 500 nM for 15 min at 32 °C. Control samples contained 1% ethanol. The enzymatic reaction was started by addition of [^{14}C]-deoxycorticosterone (60 mCi/mmol; NEN, Boston, MA) in a final concentration of 100 nM. Sample tubes were shaken horizontally at 32 °C for 6 h. The enzyme reaction was quenched by the addition of the same volume of ethyl acetate to extract the steroids. The organic layer was pipetted into a fresh cup and evaporated to dryness. The residue was dissolved in 10 μL of chloroform and the conversion of the substrate into corticosterone was analyzed by HPTLC as described in section 5.

4. Activity and Selectivity Assay Using V79 Cells. V79 MZh 11B1 and V79 MZh 11B2 cells were grown on 24-well cell culture plates with 1.9 cm^2 culture area per well (Nunc, Roskilde, Denmark) until confluence. Before testing, the DMEM culture medium was removed and 400 μL of fresh DMEM, containing the inhibitor in at least three different concentrations for determining the IC_{50} value, was added to each well. After a preincubation step of 60 min at 37 °C, the reaction was started by the addition of 100 μl of DMEM containing the substrate 11-deoxycorticosterone (20 μM, containing 6 nCi of [4-^{14}C]11-deoxycorticosterone, dissolved in ethanol). The V79 MZh 11B1 cells were incubated for 120 min, whereas the V79 MZh 11B2 cells were incubated for 40 min. Controls were treated in the same way without inhibitor. Enzyme reactions were stopped by extracting the supernatant with ethyl acetate. Samples were centrifuged, and the solvent was pipetted into fresh cups. The solvent was evaporated, and the steroids were redissolved in 10 μL of chloroform and analyzed by HPTLC.

5. HPTLC Analysis and Phosphoimaging of Radiolabeled Steroids. The redissolved steroids were transferred onto a HPTLC plate (20 cm × 10 cm, silica gel $60F_{254}$) with concentrating zone (Merck, Darmstadt, Germany) and developed two times using the solvent chloroform/methanol/water (300:20:1). For the CYP11B2 reaction in V79 MZh 11B2, unlabeled 11-deoxycorticosterone, corticosterone, 18-hydroxycorticosterone and aldosterone were used as references. Subsequently, imaging plates (BAS MS2340, for ^{14}C samples, Raytest, Straubenhardt, Germany) were exposed to the HPTLC plates for 48 h. The imaging plates were scanned using the phosphoimager system Fuji FLA 3000 (Raytest, Straubenhardt, Germany), and the steroids were quantified using the software AIDA (Raytest, Straubenhardt, Germany).

6. Inhibition of Human Hepatic CYPs. Compound **5** was tested for inhibition of human hepatic CYP3A4 and CYP2D6 using concentrations corresponding to the IC_{50} values of the well-known inhibitors ketoconazole and quinidine, respectively. The recombinantly expressed enzymes in baculovirus-infected insect microsomes (Supersomes) were used and the manufacturer's instructions were followed (www.gentest.com).

7. Protein Modeling and Docking. Using the recently resolved human cytochrome CYP2C9 structure (PDB code: 1OG5)[44] as template, a homology model was build and refined for CYP11B2.[17,18] In this study, selected compounds (Table 2) were docked into the refined homology model using FlexX-Pharm.[45] Pharmacophore constraints were applied to ensure the right binding mode of the inhibitors (a Fe(heme)−N(inhibitor) interaction was required). Based on the docked protein−inhibitor complex structures, molecular dynamics simulations were performed using the GROMOS96 force field[46] and the GROMACS program.[47] A cutoff of 14 Å was used for the nonbonded interactions, and a time step of 1 fs was applied. The temperature was maintained by weak coupling to an external bath with a temperature coupling relaxation time of 0.1 ps.[48] Throughout the simulations the bond lengths were constrained to ideal values using the LINCS procedure. No explicit solvent was included, because of the mainly hydrophobic character of the binding pocket. Potential solvent molecules were approximated through a dielectric constant of 4.0. Harmonic restraints were applied to all backbone atoms outside the binding pocket (all residues, except residues 106−133, 212−221, 244−262, 305−332, 372−384, and 483−494). The systems were heated from 0 to 300K over 200 ps and afterward 800 ps of molecular dynamics were performed at 300 K.

8. Caco-2 Transport Experiments. Caco-2 cell culture and transport experiments were performed according to Yee[34] with small modifications. Cell culture time was reduced to 10 days by increasing seeding density from 6.3×10^4 to 1.65×10^5 cells per well. Four reference compounds, atenolol, ketoprofene, testosterone and erythromycin, were used in each assay for validation of the transport properties of the Caco-2 cells. The compounds were applied to the cells as mixtures (cassette dosing) to increase the throughput of the permeability tests. The starting concentration of the compounds in the donor compartment was 50 μM in buffer containing either 1% ethanol or DMSO. After a preincubation step of 20 min at 37 °C, the reaction was started. The 12-well Transwellplates (Corning Costar) were stirred (20 rpm) at 37 °C. Samples were taken from the acceptor side after 60, 120 and 180 min and from the donor side after 0 and 180 min. Each experiment was run in triplicate. Monolayer integrity was checked by measuring the transepithelial electrical resistance (TEER) before the transport experiments and by measuring lucifer yellow permeability after each assay. All samples were analyzed by LS-MS/MS after 1:1 dilution with buffer of the opposite

transwell chamber containing 2% acetic acid. The apparent permeability coefficients (P_{app}) were calculated using the equation $P_{app} = dQ/dt \cdot A \cdot c_0$, where dQ/dt is the mass appearance rate in the acceptor compartment, A is the surface area of the transwell membrane, and c_0 is the initial concentration in the donor compartment.

9. Metabolic Stability Assay. The assay was performed with rat microsomes (male pool, Gentest, Woburn, MA). The incubation solution contained a microsomal suspension of 0.15 mg of protein per mL in phosphate buffer 0.1 M, pH 7.4, and a NADPH-regenerating system (NADP 1 mM, glucose-6-phosphate 5 mM, glucose-6-phosphate dehydrogenase 5 U/mL, $MgCl_2$ 5 mM). After preincubation at 37 °C, the reaction was initiated by the addition of the test compound (a stock solution of 10 mM in 100% DMSO, diluted in phosphate buffer 0.1 mM, pH 7.4 to reach the final concentration of 5 μM with 2% of final DMSO concentration). After 0, 30, 60, 120 and 180 min, 200 μL from the incubation was removed and added to ethyl acetate, containing the internal standard methoxyverapamil (5 μM), to stop the reaction. Subsequently, the samples were vortexed for 5 min, the organic layer evaporated in a vacuum centrifuge, reconstituted in mobile phase and analyzed by LC-MS/MS. The percentage of the remaining test compound was plotted against the corresponding time points, and the half-life time was derived by a standard fit of the data.

10. Metabolite Detection. The metabolites were identified by comparison of the total ion chromatograms between the incubation of time point zero and after 180 min. Once quasi-molecular ions were detected, they were subjected to further MS/MS analysis. The product ion MS/MS spectra of the parent compound was subsequently compared with the corresponding fragmentation pattern of putative metabolite structures. The specific fragment ion that showed a shift in its *m/z* was used to metabolite identification.

Acknowledgment. We thank the Deutsche Forschungsgemeinschaft (Ha 1513/6), the Saarland Ministry of Education, Culture and Science (ETTT Project) and the Fonds der Chemischen Industrie for financial support. We thank Ms. Anja Palusczak and Ms. Martina Palzer for their help in performing the in vitro tests. Thanks are due to Professor Rita Bernhardt, Saarland University and Organon, Oss, The Netherlands, for supplying the V79 cells.

Supporting Information Available: Analytical and spectroscopic data of synthesized compounds **5i**−**7i**, **9i**, **10i**, **14i**, **14ii**, **21i**, **4**−**9**, **12**−**14**, **16**, **19**−**22**, **30**, **31** and tables of elemental analyses, logP and solubility values of compounds **1**−**31**. This material is available free of charge via the Internet at http://pubs.acs.org.

References

(1) Kawamoto, T.; Mitsuuchi, Y.; Toda, K.; Yokoyama, Y.; Miyakara, K.; Miura, S.; Onishi, T.; Ichihawa, Y.; Nakao, K.; Imura, H.; Ulick, S.; Shizuta, Y. Role of steroid 11β-hydroxylase and steroid 18-hydroxylase in the biosynthesis of glucocorticoids and mineralocorticoids in humans. *Proc. Natl. Acad. Sci. U.S.A.* **1992**, *89*, 1458−1462.

(2) Brilla, C. G. Aldosterone and myocardial fibrosis in heart failure. *Herz* **2000**, *25*, 299−306.

(3) Lijnen, P.; Petrov, V. Induction of cardiac fibrosis by aldosterone. *J. Mol. Cell. Cardiol.* **2000**, *32*, 865−879.

(4) Pitt, B.; Zannad, F.; Remme, W. J.; Cody, R.; Castaigne, A.; Perez, A.; Palensky, J.; Wittes, J. The effect of spironolactone on morbidity and mortality in patients with severe heart failure. *N. Eng. J. Med.* **1999**, *341*, 709−717.

(5) Pitt, B.; Remme, W. J.; Zannad, F.; Neaton, J.; Martinez, F.; Roniker, B.; Bittman, R.; Hurley, S.; Kleiman, J.; Gatlin, M. Eplerenone, a selective aldosterone blocker, in patients with left ventricular dysfunction after myocardial infarction. *N. Eng. J. Med.* **2003**, *348*, 1309−21.

(6) Khan, N. U. A.; Movahed, A. The role of aldosterone and aldosterone-receptor antagonists in heart failure. *Rev. Cardiovasc. Med.* **2004**, *5*, 71−81.

(7) Juurlink, D. N.; Mamdani, M. M.; Lee, D. S.; Kopp, A.; Austin, P. C.; Laupacis, A.; Redelmeier, D. A. Rates of hyperkalemia after publication of the randomized aldactone evaluation study. *N. Engl. J. Med.* **2004**, *351*, 543−551.

(8) Hartmann, R. W. Selective inhibition of steroidogenic P450 enzymes: current status and future perspectives. *Eur. J. Pharm. Sci.* **1994**, *2*, 15−16.

(9) Ehmer, P. B.; Bureik, M.; Bernhardt, R.; Müller, U.; Hartmann, R. W. Development of a test system for inhibitors of human aldosterone synthase (CYP11B2): Screening in fission yeast and evaluation of selectivity in V79 cells. *J. Steroid Biochem. Mol. Biol.* **2002**, *81*, 173−179.

(10) Hartmann, R. W.; Müller, U.; Ehmer, P. B. Discovery of selective CYP11B2 (aldosterone synthase) inhibitors for the therapy of congestive heart failure and myocardial fibrosis. *Eur. J. Med. Chem.* **2003**, *38*, 363−366.

(11) (a) Hartmann, R. W.; Bayer, H.; Grün, G.; Sergejew, T.; Bartz, U.; Mitrenga, M. Pyridyl-substituted tetrahydrocyclopropa[α]-naphthalenes: Highly active and selective inhibitors of P450 arom. *J. Med. Chem.* **1995**, *38*, 2103−2111. (b) Jacobs, C.; Frotscher, M.; Dannhardt, G.; Hartmann, R. W. 1-Imidazolyl-(alkyl)-substituted di- and tetrahydroquinolines and analogues: Syntheses and evaluation of dual inhibitors of thromboxane A_2 synthase and aromatase. *J. Med. Chem.* **2000**, *43*, 1841−1851. (c) Recanatini, M.; Bisi, A.; Cavalli, A.; Belluti, F.; Gobbi, S.; Rampa, A.; Valenti, P.; Palzer, M.; Palusczak, A.; Hartmann, R. W. A new class of nonsteroidal aromatase inhibitors: Design and synthesis of chromone and xanthone derivatives and inhibition of the P450 enzymes aromatase and 17α-hydroxylase/C17,20-lyase. *J. Med. Chem.* **2001**, *44*, 672−680. (d) Leonetti, F.; Favia, A.; Rao, A.; Aliano, R.; Palusczak, A.; Hartmann, R. W.; Carotti, A. Design, synthesis and 3D QSAR of novel potent and selective aromatase inhibitors. *J. Med. Chem.* **2004**, *47*, 6792−6803.

(12) (a) Wachall, B. G.; Hector, M.; Zhuang, Y.; Hartmann, R. W. Imidazole substituted biphenyls: A new class of highly potent and in vivo active inhibitors of P450 17 as potential therapeutics for treatment of prostate cancer. *Bioorg. Med. Chem.* **1999**, *7*, 1913−1924. (b) Hartmann, R. W.; Hector, M.; Wachall, B. G.; Palusczak, A.; Palzer, M.; Huch, V.; Veith, M. Synthesis and evaluation of 17-aliphatic heterocycle-substituted steroidal inhibitors of 17α-hydroxylase/C17−20-lyase (P450 17). *J. Med. Chem.* **2000**, *43*, 4437−4445. (c) Zhuang, Y.; Wachall, B. G.; Hartmann, R. W. Novel imidazolyl and triazolyl substituted biphenyl compounds: Synthesis and evaluation as nonsteroidal inhibitors of human 17α-hydroxylase-C17,20-lyase (P450 17). *Bioorg. Med. Chem.* **2000**, *8*, 1245−1252. (d) Haidar, S.; Ehmer, P. B.; Barassin, S.; Batzl-Hartmann, C.; Hartmann, R. W. Effects of novel 17α-hydroxylase/C17,20-lyase (P450 17, CYP 17) inhibitors on androgen biosynthesis in vitro and in vivo. *J. Steroid Biochem. Mol. Biol.* **2003**, *84*, 555−562.

(13) Taymans, S. E.; Pack, S.; Pak, E.; Torpy, D. J.; Zhuang, Z.; Stratakis, C. A. Human CYP11B2 (aldosterone synthase) maps to chromosome 8q24.3. *J. Clin. Endocrinol. Metab.* **1998**, *83*, 1033−1036.

(14) Häusler, A.; Monnet, G.; Borer, C.; Bhatnagar, A. S. Evidence that corticosterone is not an obligatory intermediate in aldosterone biosynthesis in the rat adrenal. *J. Steroid Biochem.* **1989**, *34*, 567−570.

(15) Demers, L. M.; Melby, J. C.; Wilson, T. E.; Lipton, A.; Harvey, H. A.; Santen, R. J. The effects of CGS 16949A, an aromatase inhibitor on adrenal mineralocorticoid biosynthesis. *J. Clin. Endocrinol. Metab.* **1990**, *70*, 1162−1166.

(16) Bureik, M.; Hubel, K.; Dragan, C. A.; Scher, J.; Becker, H.; Lenz, N.; Bernhardt, R. Development of test systems for the discovery of selective human aldosterone synthase (CYP11B2) and 11beta-hydroxylase (CYP11B1) inhibitors. Discovery of a new lead compound for the therapy of congestive heart failure, myocardial fibrosis and hypertension. *Mol. Cell. Endocrinol.* **2004**, *217*, 249−254.

(17) Ulmschneider, S.; Müller-Vieira, U.; Mitrenga, M.; Hartmann, R. W.; Oberwinkler-Marchais, S.; Klein, C. D.; Bureik, M.; Bernhardt, R.; Antes, I.; Lengauer, T. Synthesis and evaluation of imidazolylmethylene-tetrahydronaphthalenes and imidazolylmethylene-indanes: Potent inhibitors of aldosterone synthase. *J. Med. Chem.* **2005**, *48*, 1796−1805.

(18) Ulmschneider, S.; Müller-Vieira, U.; Klein, C. D.; Antes, I.; Lengauer, T.; Hartmann, R. W. Synthesis and evaluation of (pyridylmethylene)tetrahydronaphthalenes/-indanes and structurally modified derivatives: Potent and selective inhibitors of aldosterone synthase. *J. Med. Chem.* **2005**, *48*, 1563−1575.

(19) Miyaura, N.; Suzuki, N. Palladium-catalyzed cross-coupling reactions of organoboron compounds. *Chem. Rev.* **1995**, *95*, 2457−2483.

(20) Huisgen, R.; Sorge, G. Orientating phenomena in the substitution on aromatic bicyclic compounds. III. Radical substitutions in the naphthalene group. *Liebigs Ann. Chem.* **1950**, *566*, 162−184.

(21) Ono, S.; Inoue, Y.; Yoshida, T.; Ashimori, A.; Kosaka, K.; Imada, T.; Fukaya, C.; Nakamura, N. Preparation and pharmacological evaluation of novel glycoprotein (Gp) IIb/IIIa antagonists. 1. The selection of naphthalene derivatives. *Chem. Pharm. Bull.* **1999**, *49*, 1685−1693.
(22) Mewshaw, R. E.; Edsall, R. J.; Yang, C.; Harris, H. A.; Keith, J. C.; Albert, L. M. (Wyeth). Substituted phenyl naphthalenes as estrogenic agents. Patent WO03051805, 2003.
(23) Young, T. E.; Amstutz, E. D. Halogen reactivities. Certain heterocyclic iminohalide systems. *J. Am. Chem. Soc.* **1951**, 4773−4775.
(24) Jagdmann, G. E.; Munson, H. R.; Gero, T. W. A mild efficient procedure for the conversion of carboxylic acid esters to primary amides using formamide/methanolic sodium methoxide. *Synth. Commun.* **1990**, *20*, 1203−1208.
(25) Lam, P. Y. S.; Clark, C. G.; Saubern, S.; Adams, J.; Winters, M. P.; Chan, D. M. T.; Combs, A. New aryl/heteroaryl C−N bond cross-coupling reactions via arylboronic acid/cupric acetate arylation. *Tetrahedron Lett.* **1998**, *39*, 2941−2944.
(26) Lan, J.; Chen, L.; Yu, X.; You, J.; Xie, R. A simple copper salt catalysed the coupling of imidazole with arylboronic acids in protic solvent. *Chem. Commun.* **2004**, *2*, 188−189.
(27) Bredereck, H.; Theilig, G. Imidazolsynthesen mit Formamid. *Chem. Ber.* **1953**, *86*, 88−96.
(28) Denner, K.; Doehmer, J.; Bernhardt, R. Cloning of CYP11B1 and CYP11B2 from normal human adrenal and their functional expression in COS-7 and V79 chinese hamster cells. *Endocr. Res.* **1995**, *21*, 443−448.
(29) Thompson, E. A.; Siiteri, P. K. Utilization of oxygen and reduced nicotinamide adenine dinucleotide phosphate by human placental microsomes during aromatization of androstenedione. *J. Biol. Chem.* **1974**, *249*, 5364−5372.
(30) Hartmann, R. W.; Batzl, C. Aromatase inhibitors. Synthesis and evaluation of mammary tumor inhibiting activity of 3-alkylated 3-(4-aminophenyl)piperidine-2,6-diones. *J. Med. Chem.* **1986**, *29*, 1362−1369.
(31) Ehmer, P. B.; Jose, J.; Hartmann, R. W. Development of a simple and rapid assay for the evaluation of inhibitors of human 17α-hydroxylase-$C_{17,20}$-lyase (P450c17) by coexpression of P450c17 with NADPH-cytochrome-P450-reductase in *Escherichia coli*. *J. Steroid Biochem. Mol. Biol.* **2000**, *75*, 57−63.
(32) Hutschenreuter, T. U.; Ehmer, P. B.; Hartmann, R. W. Synthesis of hydroxy derivatives of highly potent nonsteroidal CYP17 inhibitors as potential metabolites and evaluation of their activity by a non cellular assay using recombinant enzyme. *J. Enzyme Inhib. Med. Chem.* **2004**, *19*, 17−32.
(33) Hidalgo, I. J. Assessing the absorption of new pharmaceuticals. *Curr. Top. Med. Chem.* **2001**, *1*, 385−401.
(34) Yee, S. In vitro permeability across Caco-2 cells (colonic) can predict in vivo (small intestinal) absorption in men − fact or myth. *Pharm. Res.* **1997**, *14*, 763−766.
(35) Tannergren, C.; Langguth, P.; Hoffmann, K. J. Compound mixtures in Caco-2 cell permeability screens as a means to increase screening capacity. *Pharmazie* **2001**, *56*, 337−342.
(36) Laitinen, L.; Kangas, H.; Kaukonen, A. M.; Hakala, K.; Kotiaho, R.; Kostiainen, R.; Hirvonen, J. N-in-one permeability studies of heterogeneous sets of compounds across Caco-2 cell monolayers. *Pharm. Res.* **2003**, *20*, 187−197.
(37) Saito, H.; Fukasawa, Y.; Otsubo, Y.; Yamada, K.; Sezaki, H.; Yamashita, S. Carrier-mediated transport of macrolide antimicrobial agents across Caco-2 cell monolayers. *Pharm. Res.* **2000**, *17*, 761−765.
(38) Belkina, N. V.; Lisurek, M.; Ivanov, A. S.; Bernhardt, R. Modelling of three-dimensional structures of cytochromes P450 11B2 and 11B1. *J. Inorg. Biochem.* **2001**, *87*, 197−207.
(39) Chowdhury, S.; Georghiou, P. E. Palladium catalyzed cross-coupling between phenyl- or naphthylboronic acids and benzylic bromides. *Tetrahedron Lett.* **1999**, *40*, 7599−7603.
(40) Li, W.; Nelson, D. P.; Jensen, M. S.; Hoerrner, R. S.; Cai, D.; Larsen, R. D.; Reider, P. J. An improved protocol for the preparation of 3-pyridyl- and some arylboronic acids. *J. Org. Chem.* **2002**, *67*, 5394−5397.
(41) Kauffmann, T.; Tigler, D.; Woltermann, A. Kondensation von 3-(1-Imidazolyl)- und -(1-Benzimidazolyl)-chinolin zu Heterocyclotetraaromaten. *Chem. Ber.* **1982**, *115*, 452−458.
(42) Kajigaeshi, S.; Kakinami, T.; Okamoto, T.; Fujisaki, S. Synthesis of bromoacetyl derivatives by use of tetrabutylammonium tribromide. *Bull. Chem. Soc. Jpn.* **1987**, *60*, 1159−1160.
(43) Dahn, H.; Zoller, P. Über die katalytische Hydrogenolyse von Derivaten des *p*-Phenylbenzylamins. *Helv. Chim. Acta* **1952**, *35*, 1348−1351.
(44) Williams, P. A.; Cosme, J.; Ward, A.; Angove, H. C.; Matak Vinkovic, D.; Jhoti, H. Crystal structure of human cytochrome P4502C9 with bound warfarin. *Nature* **2003**, *424*, 464−468.
(45) Hindle, S. A.; Rarey, M.; Buning, C.; Lengauer, T. Flexible docking under pharmacophore type constraints. *J. Comput. Aided Mol. Des.* **2002**, *16*, 129−149.
(46) Scott, W. R. P.; Hünenberger, P. H.; Tironi, I. G.; Mark, A. E.; Billeter, S. R.; Fennen, J.; Torda, A. E.; Huber, T.; Krüger, P.; van Gunsteren, W. F. The GROMOS Biomolecular Simulation Program Package. *J. Phys. Chem. A* **1999**, *103*, 3596−3607.
(47) Lindahl, E.; Hess, B.; van der Spoel, D. GROMACS 3.0: a package for molecular simulation and trajectory analysis. *J. Mol. Mod.* **2001**, *7*, 306−317.
(48) Berendsen, H. J. C.; Postma, J. P. M.; van Gunsteren, W. F.; Hermans, J. Interaction models for water in relation to protein hydration. In *Intermolecular Forces*; Pullman, B., Ed.; Reidel Publishing Co.: Dordrecht, 1981; pp 331−342.

JM0503704